International Journal of Advanced Technology and Engineering Exploration, Vol 9(97)
ISSN (Print): 2394-5443 ISSN (Online): 2394-7454
http://dx.doi.org/10.19101/IJATEE.2021.876118

Research Article

Evaluation of polycaprolactone/carboxymethylcellulose scaffolds using hyperelastic model

Noppadol Sriputtha[1*], Fasai Wiwatwongwana[1] and Nattawit Promma[2]
Department of Advanced Manufacturing Technology, Pathumwan Institute of Technology, Bangkok, Thailand[1]
Department of Mechanical Engineering, Chiang Mai University, Chiang Mai, Thailand[2]

Received: 06-June-2022; Revised: 28-November-2022; Accepted: 01-December-2022

Abstract
Tissue engineering is an interesting field. The tissue engineering scaffold allows the delivery of cells and growth factors to the damaged part of the body to allow for the regeneration of tissue. This work aimed to evaluate polycaprolactone (PCL) blended with carboxymethylcellulose (CMC) composite scaffolds. The porous scaffolds were created using the salt leaching process. An experimental technique was used to characterize the mechanical characteristics of the scaffolds. We evaluated the modeling by describing the stress-strain behavior of the scaffolds using the neo-Hookean model. The shear modulus of the polycaprolactone scaffold containing 2, 11, 15.5, and 20% CMC was 0.074, 0.037, 0.034, and 0.085 megapascal (MPa), respectively. A scaffold with a PCL/CMC ratio of 93.5/6.5 had the highest average shear modulus of 0.245 MPa when compared to other mixed scaffolds. There was a significant difference when compared to a pure polycaprolactone scaffold. The result could provide excellent conditions for creating scaffolds for use in cell transplantation and culture.

Keywords
Polycaprolactone, Carboxymethylcellulose, Compressive modulus, Shear modulus, Neo-hookean model.

1.Introduction
The skin represents an efficient barrier that protects organisms from physical and chemical attacks [1]. Damage or loss of tissue or body part is often one of the deadly and costly problems in medical care [2, 3]. Tissue engineering (TE) has increased in significance because of the need to combine or apply multi-skilled methods for resolving this medical challenge [4]. The goal of TE is to replace or restore damaged tissue by employing artificial constructions that control the development of new tissue. This discipline combines knowledge from biology, materials science, engineering, and clinical sciences. It opens up new avenues for treating patients with illnesses and accidents affecting tissues such as bone, cartilage, skin, nerves, and even blood vessels [5, 6].

TE uses biodegradable polymer scaffolds such as Polycaprolactone (PCL), poly-l-lactic acid (PLLA), and polylactic glycolic acid (PLGA) to promote cells until the extracellular matrix (ECM) regenerated them [7, 8].

PCL, another approved biocompatible and bioresorbable polyester with promising medical applications [9], It is a biodegradable polymer currently being developed as the material for scaffolds in TE [10].

PCL is an aliphatic polyester that is linear. It is an easy-to-process, hydrophobic, biocompatible, semi-crystalline polymer that degrades slowly [11–15]. For this reason, we present a PCL composite base material with adjustable hydrophilicity. It achieved this variable hydrophilicity by offering highly hydrophilic biocompatible compounds such as carboxymethylcellulose (CMC) [16]. CMC has strong mechanical qualities such as high viscosity and shear strength, which can enhance the scaffold's mechanical integrity [17–21]. CMC is the main structural and functional component of three-dimensional (3D) printed scaffolds used by Diaz-gomez et al. [22] for the healing of diabetic wounds. CMC scaffolds improved re-epithelialization, granulation, and angiogenesis in full-thickness skin defects. CMC is regarded as an excellent component of active dressings for diabetic wounds. As a result,

*Author for correspondence

CMC is qualified for use as an ingredient to improve PCL in this study.

Key functions of the scaffold are proper strength to support, compression and tensile strength during transplantation, proper pore size to allow the migration and growth of fibroblasts within the scaffold, and cell biocompatibility and biodegradation. Scaffolds behavior usually exhibits a non-linear stress-strain response because of elastomer behavior. It remains difficult to identify the material parameters that govern the constitutive equation system. Various biomaterials have benefited from the application of hyperelastic models [23]. As a result, a basic hyperelastic material model, especially the neo-Hookean model, can describe the constitutive behavior of the scaffold. Curve fitting from a homogeneity test or uniaxial compression test can determine scaffold construction parameters [24, 25].
The hyperelastic model with a neo-Hookean model is presented in this study, along with a compressive modulus for researching shear modulus with a neo-Hookean model. To effectively simulate the results, a MATLAB R2021b is used. The proposed materials' experimental examination (PCL blended with CMC; PCL/CMC) was carried out on a uniaxial universal testing machine (UTM), and the findings were analyzed and compared to pure polycaprolactone, which showed enhanced performance.

Our motivation of this research was to use PCL and CMC because of benefit cheap and available and use hyperalastic model for evaluated mechanical property of composite scaffold for benefit further works and medical applications.

The structure of the paper is as follow: The research effort linked to the field of study is presented in section two. The proposed prediction model for hyperelastic materials use a neo-Hookean concept. Section 3 explains how to make porous scaffolds and how to test them. The exploratory data analysis, performance analysis, and outcomes comparison are presented in sections 4 and 5. Finally, the study brings the topic to a close by, making recommendations for further research.

2.Literature review

Researchers have proposed several study approaches for the idea of material deformation. A hyperelastic model, such as the neo-Hookean, Mooney-Rivlin, Ogden, and Yeoh models, is used to study the behavior of material deformation. The neo-Hookean model is a well-known one for predicting material deformation behavior.

Dong and Duan [26] proposed using the finite element method (FEM) to distinguish the analysis of elastic and hyperelastic materials. They investigated the hyperelastic parameters of the Yeoh, Mooney-Rivlin, and neo-Hookean models based on a uniaxial tensile test. The Yeoh model displayed the results of the hyperelastic models with the lowest residual sum of squares (RSS) for hydrogenated nitrile butadiene rubber (HNBR). However, they suggested that more care should be taken when choosing a suitable material model and an analysis technique for evaluation.

Anssari-benam et al. [27] proposed inflating incompressible rubber-like spherical and cylindrical shells with a newly generalized neo-Hookean strain energy function. Their research would show the model's ability to detect differing uncertainty phenomena in the inflation of rubber-like materials, namely the limit-point and inflation-jump instabilities.

Simon et al. [28] proposed the mechanical characterization of adhesives with hyperelastic behavior by using rubber as a specimen whose behavior is similar to that of highly flexible adhesives. A test plan was carried out on simple specimens in uniaxial and planar configurations, designed to measure the non-linear behavior of the adhesives in both tension and shear. Subsequently, using finite element models (FEM) of the tested specimens, different behavioural laws from those usually used for the representation of hyperelastic materials are tested. The result has been determined to be that the Mooney-Rivlin model was the one that allows the best fit and therefore might be the most suitable to represent the behavior of hyperelastic adhesives.

Kar et al. [29] investigated the mechanical behavior of a displaced axially slightly compressible neo-Hookean fiber embedded in a slightly compressible generalized neo-Hookean matrix. They looked at how material and geometric parameters affected the force needed to axially displace the fiber, shear stress at the interface and within the fiber-matrix system, and the Green-St. Venant strain norm. The results revealed as an intriguing result in which the maximum shear stress occurs in the matrix's interior when the shear modulus of the fiber is comparable to that of the matrix. Furthermore, as the fiber and matrix became

more compressible, the maximum shear stress decreased.

Cheng and Zhang [23] offer a framework for a general procedure to extract the stress and elasticity for hyperelastic models. The specific differences between the formulas used in the displacement formulation and the mixed displacement and pressure formulation are described throughout the derivation. Three hyperelastic models, Mooney–Rivlin, Yeoh, and Ogden, are provided as examples. They cover the scope from isotropic to anisotropic materials and first order to higher orders. These in-depth derivations are validated using numerical tests that demonstrate excellent agreement with analytical and other computational. Any hyperelastic model can be quickly developed using this architecture as user-defined functions in a software application or from start as original source code.

Wiwatwongwana and Chaijit [24] proposed using the freeze-drying method to create a gelatin-CMC scaffold with various ratios. Using universal testing equipment, a compressive test was done to characterize the scaffold mechanically. The data was used to calculate compressive and shear modulus, which were then investigated using a neo-Hookean model. The deformed scaffold and total strain energy time response were investigated using a FEM. The findings could point to the ideal conditions for scaffold manufacturing based on mechanical analysis, which could be useful in TE.

Chen et al. [30] established a new constitutive model to predict the effective mechanical behavior of incompressible neo-Hookean materials under finite deformation. The results indicated that the suggested constitutive model could give reliable estimates of the mechanical behavior of the porous neo-Hookean materials. The findings indicated that their model could better reflect overall mechanical behavior than the comparable model.

Raheem and Al-mukhtar [31] suggested looking into the strain energy density function in order to identify a suitable constitutive model that adequately describes the nonlinear behavior of biomaterials in unconfined compression tests. They employed hyperelastic models like Ogden, neo-Hookean, Mooney-Rivlin, and Yeoh to fit the experimental data for their materials. Therefore, finite element analysis (FEA) with ABAQUS/CAE is employed to evaluate the efficacy of the hyperelastic models to forecast the nonlinear behavior of biomaterials in tension and to validate the hyperelastic models in compression. The FEA predicted findings matched the test data, and all hyperelastic models met the experimental data.

Liu and Moran [32] proposed in a neo-Hookean sheet, reinforced by two families of nonlinear fibers, where the fibers are characterized using the conventional reinforcing model, they offered a study of asymptotic fracture tip fields. The mechanical behavior at the crack tip is dominated by fibers with higher stiffness than the matrix in the asymptotic analysis, which simplifies the analysis. Their research shows that the scenario with two types of fibers has a higher stress value than the situation with a single type of fiber.

Plotnikov [33] devised a mathematical model for incompressible neo-Hookean material volumetric growth. This type of model is used to represent the evolution of the human brain because of an external pressure. The behavior of solutions is investigated when the time variable approaches infinity. The key finding is that material changes resulting from a brief increase in pressure (hydrocephalus) are irreversible.

Zheng and Cai [34] Shengqiang were looking for analytical methods to predict cavities expanding in a compressible hyperelastic material. For the material in the formulation, they adopt a widely recognized compressible neo-Hookean hyperelastic model. They define the ratio of the Lame's first parameter and the shear modulus as a minimal dimensionless factor, assume the bulk modulus is much larger than the shear modulus of the solid, and use the traditional perturbation approach to obtain analytical methods. The impact of material compressibility on cavitation using analytical techniques is also considered. In their article, they compared the exact numerical methods and the analytical methods.

Shao et al. [35] investigated how aging foam rubber affects the material's properties and constitutive theories. They also discuss how aging affects parameters of the model and typical hyperelasticity constitutive models. The two types of constitutive models are phenomenological constitutive models and thermodynamic statistical constitutive models. The hyperelastic models are all popular phenomenological constitutive models. Numerical fitting approaches are currently mostly utilized to investigate changes in constitutive model parameters over time. As a result, they present typical hyperelastic constitutive models and the impact of aging on model parameters.

Based on the reviews it can be concluded that using a hyperelastic model can develop an evaluating hyperelastic model such as Neo-Hookean.

3.Method

3.1Materials and scaffolds fabrication

The creation procedure of PCL/CMC scaffolds was the same as in earlier studies (4). The PCL was purchased from Sigma-Aldrich, USA, and has a molecule weight (Mw) and melting temperature of 45,000 g/mol and 56–64°C, respectively. The medium viscosity CMC was obtained from Sigma-Aldrich, USA, whereas the porogen agent was a sodium chloride (NaCl) that was obtained from Merck KGaA, Germany. The solvent for these composite polymers was trifluoroethanol (TFE), which was obtained from Sigma-Aldrich, USA. The scaffolds were constructed using the salt leaching technique. To prepare polymer solutions, combine PCL pellets with CMC (PCL/CMC) and TFE at a 30% (mass) PCL solution (3g PCL + 7g TFE) [36]. We prepared scaffolds with six different PCL/CMC ratios: 100/0, 98/2, 93.5/6.5, 89/11, 84.5/15.5, and 80/20 *Table 1* shows the various ratios in which it mixed the PCL solution with the CMC.

Table 1 PCL mixed with CMC in weight ratio

Sample No.	PCL (g.)	CMC (g.)	PCL/CMC (%)
P0	6.00	0	100/0
P1	5.88	0.12	98/2
P2	5.61	0.39	93.5/6.5
P3	5.34	0.66	89/11
P4	5.07	0.93	84.5/15.5
P5	4.80	1.20	80/20

Briefly, to create the PCL/CMC scaffolds, the PCL pallets were melted at 55–65°C on a stirrer, then TFE solvent was added to make a 30% PCL solution. After adding the CMC and agitating until it is homogeneous, add the NaCl to the solution. It poured the liquid into a Teflon mold, resulting in 20 mm cube molds side by side. Allow the molds to dry overnight in a ventilated hood, then immerse the salt particles in deionized water (DI water) for two days to leach out the solvent [37]. After two days of air drying, the scaffolds were placed in a desiccator for the next stage. The prepared salt leaching PCL/CMC scaffolds showed a strongly interconnected porous network.

3.2PCL/CMC characterization

3.2.1Compression test

We typically made this scaffold using a particle salt leaching approach to create a porous structure. *Figure 1* depicts examples of PCL/CMC scaffolds. To determine the relationship between stress and strain, it collected data from experimental tests with a testing machine model Zwick/Roell Z1.0. In dry conditions at room temperature, the compression value was 0.5 mm/minute. The PCL/CMC scaffolds tested were evaluated into six blends: 100/0, 98/2, 93.5/6.5, 89/11, 84.5/15.5, and 80/20. We cut the scaffold specimens into rectangular pieces 10 mm long, 10 mm wide, and approximately 3 mm thick [4]. The strain in the scaffolds ranged from 7% to 25%, as shown by the first compressive stress-strain curve used to calculate the compressive modulus and average standard deviation (n=5). The initial shear modulus of each scaffold was predicted using a neo-Hookean model based on the raw data of the compressive modulus. The significant difference between each blending composition was determined using a student t-test with a 95% confidence interval. When the $p<0.05$ level was used, it considered the differences statistically significant.

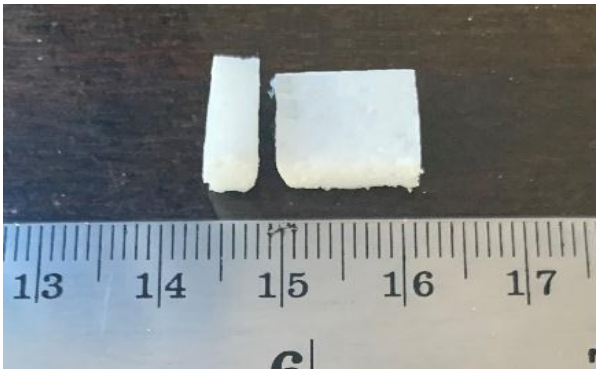

Figure 1 a test specimen of PCL/CMC scaffold

3.2.2Hyperelastic material models of PCL/CMC

Theory of hyperelastic models

We planned the nonlinear behavior of elastomeric materials at large deformations with hyperelastic material models implemented in the finite element software. The correlation between stress and strain in this situation is given by the strain energy density function (W), as opposed to linear elastic materials, where the elastic modulus and Poisson's ratio provide that correlation. The stress-strain relationship of elastic and hyperelastic materials is depicted in *Figure 2*.

In addition, hyperelastic materials can build nonlinear constitutive models based on the first, second, and third invariants (I_1, I_2, and I_3), e.g., the neo-Hookean, Mooney-Rivlin, and Yeoh models. [25, 38] However, the neo-Hookean model provided the greatest fit

since it requires one fit parameter and calculated to provide physical meaning to the fit parameter [39]. As a result, we appied the model to describe the nonlinear stress-strain relationship of the PCL/CMC composite scaffolds.

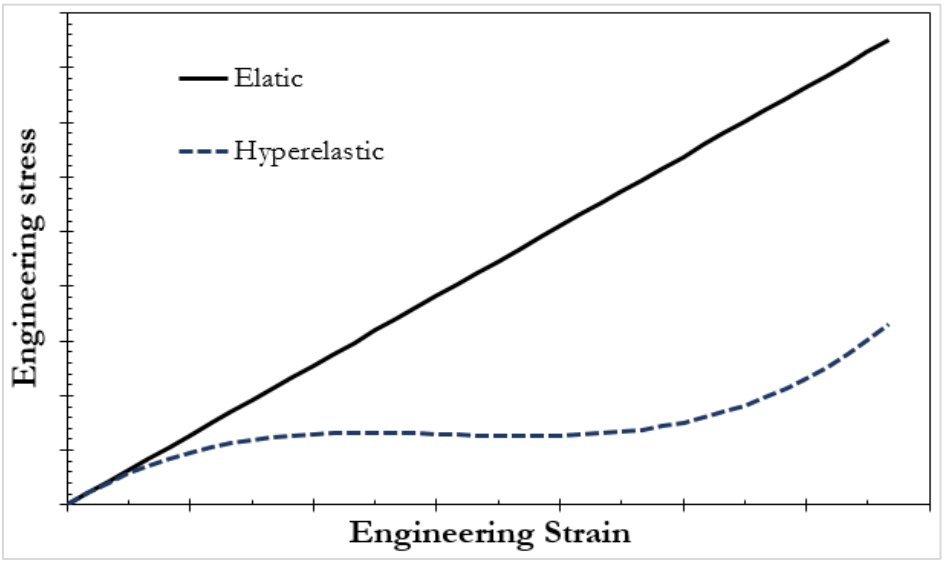

Figure 2 Stress-strain curves of hyperelastic and elastic materials [38]

The green deformation tensor's invariants are the invariants of I_1, I_2, and I_3. As demonstrated in Equation 1 to 4, these invariants may be represented with regarding to the primary stretch ratios of λ_1, λ_2, and λ_3.

$$I_1 = \lambda_1^2 + \lambda_2^2 + \lambda_3^2 \quad (1)$$

$$I_2 = \lambda_1^2\lambda_2^2 + \lambda_1^2\lambda_3^2 + \lambda_2^2\lambda_3^2 \quad (2)$$

$$I_3 = \lambda_1^2\lambda_2^2\lambda_3^2 \quad (3)$$

Where λ is the stretch ratio associated with the strain (ε) as defined by the following expression;

$$\lambda = 1 + \varepsilon \quad (4)$$

For incompressible materials, the third invariant, $I_3 = 1$. Elongation ratios λ_1, λ_2, and λ_3 are determined using elastomer tests, which include the uniaxial test, the equibiaxial test, and the planar test [38]. According to Ogden's (1972) [40] uniaxial tension and compression, $\lambda_1 = \lambda$ is the elongation ratio in the elongation direction, and $\sigma_1 = \sigma_S$ is the stress. Two of the principal stresses in equibiaxial tension/compression are equal, for instance, $\sigma_2 = \sigma_3 = \sigma_E$ whereas $\sigma_1 = 0$. The corresponding stretches are $\lambda_2 = \lambda_3 = \lambda$ whereas $\lambda_1 = \lambda{-}2$. In planar tension/compression, one of the principal extension ratios, say $\lambda 3 = 1$ is held constant [41]. Both I_1 and I_2 influence the constitutive models of these testing data. In this work, we have focused on the determination of material properties of incompressible materials by uniaxial tests. As a result, it stated the three main stretch ratios as $\lambda_1 = \lambda$, $\lambda_2 = \lambda_3 = \lambda^{0.5}$ and $\lambda = 1 + \varepsilon$. As a result, it expressed the three invariants in Equation 5 and 6.

$$I_1 = \lambda^2 + 2\lambda^{-1} \quad (5)$$

$$I_2 = 2\lambda + \lambda^{-2} \quad (6)$$

The curve fitting technique

A hyperelastic model using a neo-Hookean potential function to represent the constitutive law of hyperelastic material was used to fit the data distribution from the stress-strain relationship [25–42] Equation 7 shows the relation used to compute the G value.

$$T = G\left((1+\varepsilon) - \frac{1}{(1+\varepsilon)^2}\right) \quad (7)$$

Where T is the engineering stress, G represents the initial shear modulus, and ε is the strain.

Scaffolds' nonlinear stress-strain relationship was previously recognized as nonlinear deformation behavior. Incompressibility refers to the fact that hyperelastic materials have very low compressibility. Using strain energy potentials, it frequently predicted the constitutive properties of hyperelastic materials

(W). The derivative of the strain energy, which is a scalar function of the strain, produces the stress element. It can represent their relationship as follows [25, 42] Equation 8. :

$$\sigma_i = 2\left(\left(\lambda_i^2 - \lambda_j^2\right)\frac{\delta W}{\delta I_1} - \left(\frac{1}{\lambda_i^2} - \frac{1}{\lambda_j^2}\right) - \frac{\delta W}{\delta I_2}\right) \quad (8)$$

Where, σ, W, λ, and I stood for a Cauchy stress tensor, a strain energy function, the principal strain, and the principal invariant, respectively. The neo-Hookean model is applicable to rubber-like materials with a linear initial range and is based on the statistical thermodynamics of cross-linked polymer chains. Cross-linked polymers exhibit neo-Hookean behavior in a linear state. But eventually, the polymer chains are stretched as far as they can go by the covalent cross-links, which causes the material's elastic modulus to significantly increase. The neo-Hookean model is a well-known model for the inability to accurately predict occurrences under high stress.

Stress-strain behavior of various materials, like Hooke's law, can be simulated using neo-Hookean models for hyperelastic materials. Most materials have a linear relationship between applied stress and strain at first, but the stress-strain curve gradually becomes nonlinear. One of the most basic models is the neo-Hookean model. For an incompressible neo-Hookean material, this is the strain energy density curve [25, 43, 44] Equation 9.

$$W = C_{10}(I_1 - 3) \quad (9)$$

where C_{10} represents a material constant equal to half of the initial shear modulus (G), and the Cauchy-Green deformation tensor on the left is represented by the first invariant, I_1. The engineering stress in the fundamental expansion of an isotropic, incompressible hyperelastic material can be expressed using Equation 10.

$$T_{11} = 2\left(\lambda - \frac{1}{\lambda^2}\right).\left(\frac{\delta W}{\delta I_1} + \frac{\delta W}{\delta I_2}\right) \quad (10)$$

Therefore, the engineering stress (T_{11}) can be expressed using the following formula in terms of the neo-Hookean strain energy potential Equation 11:

$$T_{11} = G\left(\lambda - \frac{1}{\lambda^2}\right) \quad (11)$$

3.3Statistical analysis

A student t-test (n=5) with a 95% confidence interval and a $p<0.05$ level was used to determine the significance of each blending composition.

4.Result

4.1Compressive modulus

The UTM used to compress the PCL/CMC composite scaffolds to analyse the stress-strain relationship in each composition of the scaffolds. *Figure 3* showed the specimen of P2 (93.5/6.3) during the UTM compression test. It converted the force versus displacement to engineering stresses and strains using the original dimensions of each scaffold.

(a) (b) (c)

Figure 3 PCL/CMC scaffolds in the compression test (a) at the beginning, (b) during compression, and (c) at the end

As shown in *Figure 4*, scaffold cube markers represented the average compressive modulus of all scaffold conditions. The results show that the PCL scaffold has the highest compressive modulus at 6.5% CMC (P2), which is significantly different from that of the PCL-only scaffold (P0). As shown in *Table 2*, the average compressive modulus of P2 sample was 0.790 ± 0.183 MPa, while the P0 sample (100% PCL scaffold) exhibited a compressive modulus of 0.582 ± 0.106 MPa. However, the compressive modulus of other compositions (P1, P3, P4, P5) of PCL/CMC composite scaffolds exhibited a similar tendency to that of a comparative PCL scaffold (P0), with a non-significant result. However, the compressive modulus of the P3 scaffold was the lowest (0.519 ± 0.225 MPa).

4.2Shear modulus of the scaffolds

As shown in *Figure 5*, the circle markers were plotted to represent the average shear modulus of all composite scaffolds. The results revealed that the PCL composite scaffold with 6.5% CMC (P2) had the highest average shear modulus (0.245 ± 0.167 MPa) with a significantly different from the pure PCL scaffold (P0). As demonstrated in *Table 3*, the P4 sample had the lowest shear modulus of 0.034 ± 0.022 MPa Shear modulus and compressive modulus were similar in all blending compositions of PCL and CMC scaffolds.

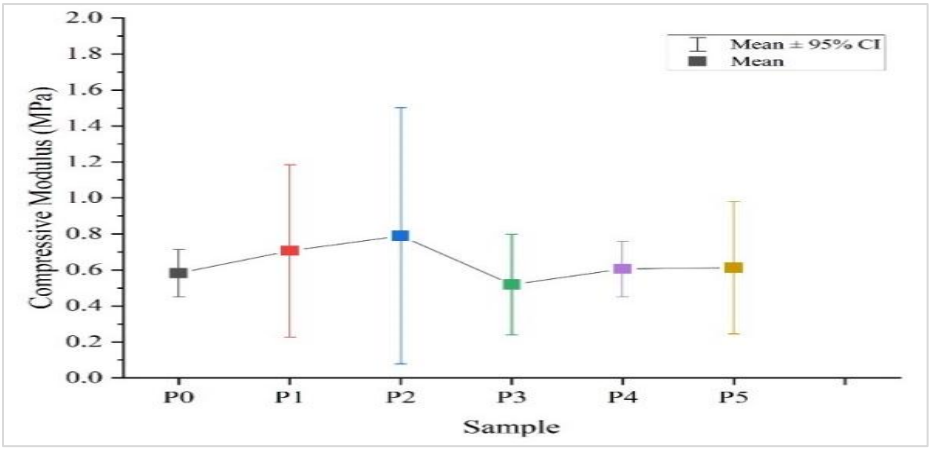

Figure 4 Compressive modulus of PCL/CMC scaffold (n=5)

Table 2 Compressive modulus of PCL/CMC scaffolds

Sample scaffolds	Compressive modulus (MPa)	Standard deviation (SD)
P0	0.582	0.106
P1	0.706	0.386
P2	0.790	0.573
P3	0.519	0.225
P4	0.605	0.124
P5	0.612	0.296

4.3Determination of constitutive parameters

We determined the scaffold's shear modulus by fitting data from the stress-strain relationship to the neo-Hookean model. The nonlinear behavior of the stress-strain relationship from compressive testing could be expressed using the neo-Hookean constitutive model [45, 46].

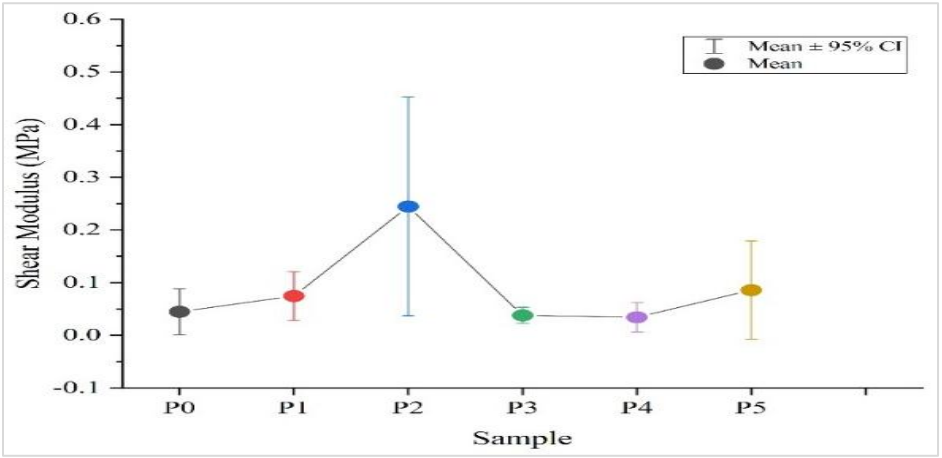

Figure 5 The PCL/CMC scaffold has an average shear modulus of 7% strain from the neo-Hookean model

Figure 6 depicts the stress-strain relationships and curve fitting of six PCL/CMC scaffold samples (P0-P5) obtained from the neo-Hookean model. The stress curves were nonlinear and represented by several points and colored lines, and the neo-Hookean curve could match the curve with a 7% strain represented by several points and a red color line. The shear modulus of each scaffold differed because the CMC content of the PCL scaffold varied. PCL blended with 6.5 percent CMC yielded the highest shear modulus. This was 0.245 ± 0.167 MPa compared to other proportions of PCL/CMC composite scaffolds. It reduced the shear modulus of the scaffold relative to the 100% PCL scaffold, which was 0.045 ± 0.035 MPa, with no significant difference from other compositions of CMC blended with the PCL scaffold. As shown in *Table 4*, the shear modulus of PCL scaffold with 2%, 11%, 15.5%, and 20% of CMC was 0.075 ± 0.0.037 MPa, 0.038 ± 0.0.012 MPa, 0.034 ± 0.022 MPa and 0.086 ± 0.075 MPa.

Table 3 The PCL/CMC scaffold has an average shear modulus of 7% strain from the neo-Hookean model

Sample scaffolds	Average shear modulus (MPa)	Standard deviation (SD)
P0	0.045	0.035
P1	0.075	0.037
P2	0.245	0.167
P3	0.038	0.012
P4	0.034	0.022
P5	0.086	0.075

Table 4 Shear modulus of the PCL/CMC scaffold using a 7% strain neo-Hookean model

Sample scaffolds	Shear modulus (MPa)	SD	R^2
P0 (0% CMC)	0.045	0.035	0.943
P1 (2% CMC)	0.075	0.037	0.890
P2 (6.5% CMC)	0.245	0.167	0.926
P3 (11% CMC)	0.038	0.012	0.978
P4 (15.5% CMC)	0.034	0.022	0.917
P5 (20% CMC)	0.086	0.075	0.938

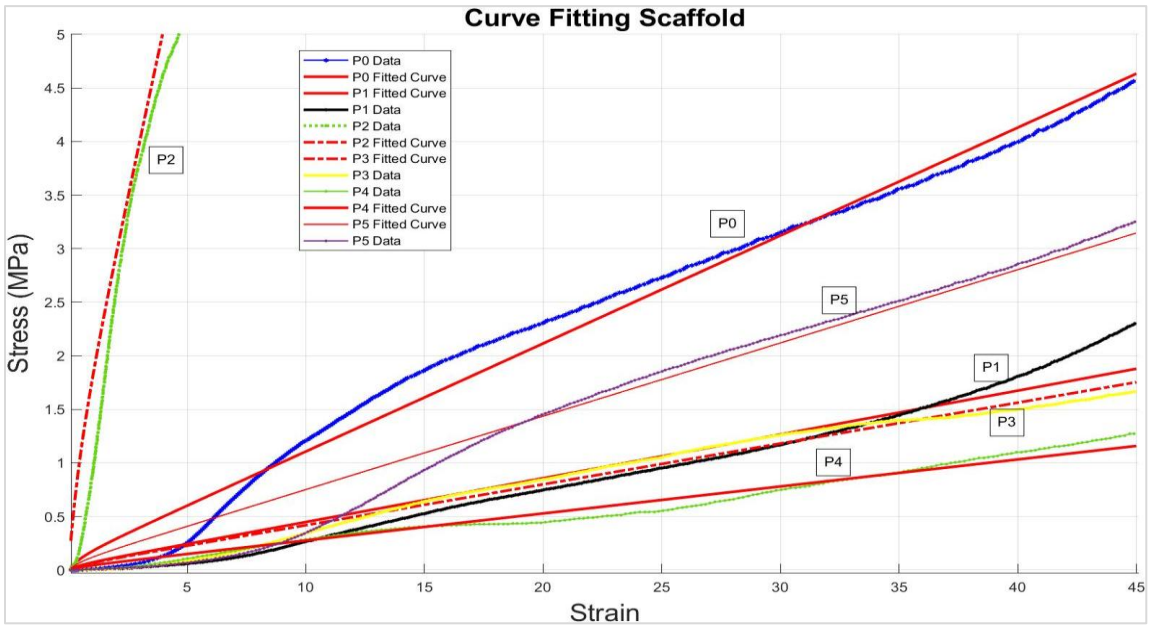

Figure 6 The stress-strain curve of a PCL/CMC scaffold and a 7% strain neo-Hookean model were used to fit it

5.Discussion

A thorough explanation of the main findings, interpretations, consequences, limits, and suggestions is provided in this section.

The average compressive modulus of all scaffold conditions is shown, same as in *Figure 5*. The findings demonstrate that the PCL scaffold has a maximum compressive modulus at 6.5%CMC (P2), which is much higher than that of the PCL only scaffold (P0). According to *Table 2*, the average compressive modulus of the P2 sample was 0.790±0.183 MPa with a maximum standard deviation, while the compressive modulus of the P0 sample (a scaffold made entirely of PCL) was 0.582±0.106 MPa with a minimum standard deviation. However, the compressive modulus of other compositions (P1, P3, P4, and P5) of PCL/CMC composite scaffolds showed a similar trend to that of a compared PCL scaffold (P0), with a non-significant result. The compressive modulus of P1, P3, P4, and P5 were 0.706, 0.519, 0.605, and 0.612, respectively. The P3 scaffold, however, has the lowest compressive modulus with a standard deviation of ±0.225 MPa. It is evident that increasing the CMC mixture will have no impact on the compressive modulus.

Figure 6 depicts the average shear modulus of all composite porous scaffolds calculated using a neo-Hookean hyperelastic model. The results revealed that the PCL composite scaffold with 6.5% CMC (P2) had the highest average shear modulus (0.245 ± 0.167 MPa). To determine the significance of each blending composition, a student t-test with a 95% confidence interval and a $p<0.05$ level was used. The PCL composite scaffold with 6.5% CMC (P2) was significantly different from the pure PCL scaffold (P0). As demonstrated in *Table 3*, the P4 sample had the lowest shear modulus of 0.034 ± 0.022 MPa. All

blending compositions of PCL and CMC scaffolds had similar shear and compressive moduli.

The mean shear modulus was plotted against the mean compressive modulus of the scaffold as shown in *Figure 7*. The blue and red lines represent the shear and compressive modulus values for all PCL/CMC scaffolds. The compressive modulus results showed that the 6.5% CMC PCL scaffold had a significant increase in compressive modulus compared to the 100% PCL scaffold.

The CMC was increased to a certain level, the viscosity of the conditions allows for the maximum shear modulus, and the compressive stress was also determined by the shear modulus. We could imply that the level is suitable for application.

We would conduct for further research on water absorption using cell culture tests in vivo and in vitro cell culture test.

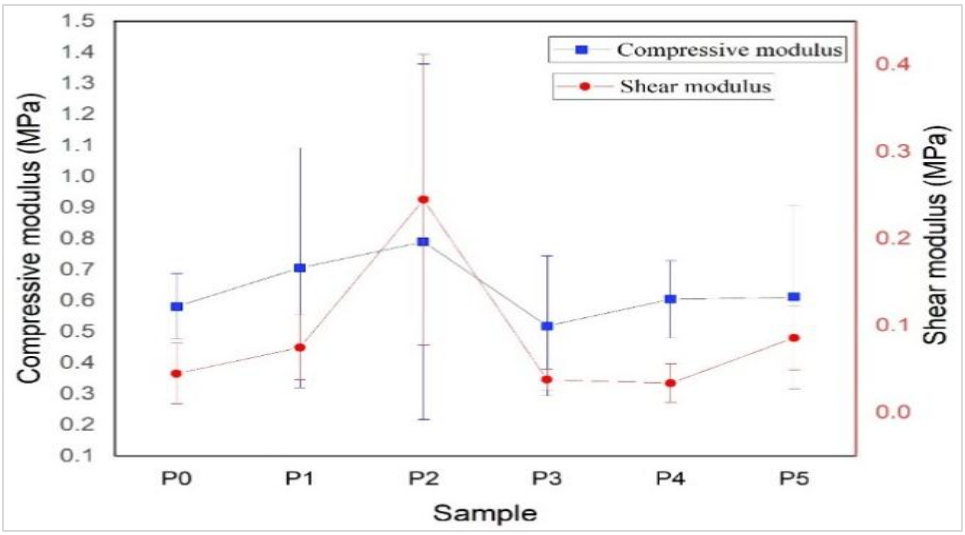

Figure 7 Compressive modulus and shear modulus in Non-linear least squares using a 7% strain neo-Hookean model

5.1Experiment and compare a neo-Hookean model

Figure 7 shows the fitting curves for the shear and compressive modulus by using the neo-Hookean constitutive model. Their data distributions follow the same pattern. The 6.5% CMC scaffold demonstrated high shear and compressive modulus. Other CMC concentrations (2%, 11%, 15.5%, and 20% CMC) added to the PCL scaffold exhibited a decrease in compressive and shear modulus when compared to the 100% PCL.

High compressive and shear modulus values, which indicate the mechanical behavior of the scaffold, offer several advantages. When immersed in the media, compressive and shear modulus values can assist it in retaining a three-dimensional porous structure. There are benefits to cultivating scaffolds for damaged patients or increasing fibroblast cells in composite scaffolds. The porous structure strength can assist cells in gaining sufficient nutrients for proliferation and growth.

5.2Limitations

The proposed research project has various restrictions, just like any other research. First, due to its small size and light weight, the test piece has a chance of moving during testing. Care must be taken to control the atmospheric conditions to prevent wind from entering the test room. Second, we used a salt particle leaching technique to create the test specimens. It's possible for salt particles to remain in the specimen if the leaching process for salt particles is inadequate. The mechanical test results for the scaffold may be distorted because of this. The last one is scaffolding preparation for molding. Because PCL is a hydrophobic material, mixing the solution requires a solvent that is compatible with both PCL and CMC, and TFE solvent was used in this work.

A complete list of abbreviations is shown in *Appendix I.*

6.Conclusion and future work

This work aimed to propose a determination of the scaffold's mechanical characteristics and the behavior of non-compressible hyperelastic materials. PCL blended with CMC in various ratios was a material that was used in this work. Uniaxial compression testing was used to determine the mechanical behavior of this material. We examined the compressive modulus with tiny deformations. The scaffold containing 6.5% CMC was the highest value (0.790 MPa) and this result was higher than the value found in the pure PCL scaffold (0.582 MPa) with a significant difference. The shear modulus of the scaffold was described in terms of an unknown variable in the neo-Hookean model. The shear modulus was obtained directly by fitting the stress-strain test data to the neo-Hookean model. The composite scaffold with 93.5% PCL and 6.5% CMC had the highest mean shear modulus (0.245 MPa). The shear modulus of scaffolds with 2%, 11%, 15.5%, and 20% CMC was decreasing, with values of 0.075, 0.038, 0.034, and 0.086 MPa, respectively. A previous study discovered that the pore size of PCL/CMC composite scaffolds was greater than that of pure PCL and that their porosity was also greater than that of pure PCL.

The results of this test with the highest shear modulus would be used for further testing. In future work, we will propose identifying characteristics that affect additional types of hyperelastic models, such as Mooney-Rivlin, Yeoh, and Ogden.

Acknowledgment

We appreciate the equipment and support provided by the Department of Advanced Manufacturing Technology, Faculty of Engineering, Pathumwan Institute of Technology.

Conflicts of interest

The authors have no conflicts of interest to declare.

Author's contributions statements

Noppadol Sriputtha: Conceptualization, experiment, investigation, data collection, writing – original draft. **Fasai Wiwatwongwana**: Conceptualization, Study conception, design, supervision, writing – original draft, writing – review and editing, analysis and interpretation of results. **Nattawit Promma**: Study conception, design, supervision, investigation on challenges and draft manuscript preparation.

References

[1] Colonna M. Skin function for human CD1a-reactive T cells. Nature Immunology. 2010; 11(12):1079-80.

[2] Laurencin CT, Nair LS. Nanotechnology and tissue engineering: the scaffold. CRC Press; 2008.

[3] Kang NU, Hong MW, Kim YY, Cho YS, Lee SJ. Development of a powder extruder system for dual-pore tissue-engineering scaffold fabrication. Journal of Bionic Engineering. 2019; 16(4):686-95.

[4] Sriputtha N, Wiwatwongwana F, Promma N. Investigation of polycaprolactone/carboxymethyl cellulose scaffolds by mechanical and thermal analysis. Engineering, Technology & Applied Science Research. 2022; 12(1):8175-9.

[5] Donate R, Monzón M, Alemán-domínguez ME. Additive manufacturing of PLA-based scaffolds intended for bone regeneration and strategies to improve their biological properties. e-Polymers. 2020; 20(1):571-99.

[6] Todros S, Todesco M, Bagno A. Biomaterials and their biomedical applications: from replacement to regeneration. Processes. 2021; 9(11):1-20.

[7] Sabzi E, Abbasi F, Ghaleh H. Interconnected porous nanofibrous gelatin scaffolds prepared via a combined thermally induced phase separation/particulate leaching method. Journal of Biomaterials Science, Polymer Edition. 2020; 32(4):488-503.

[8] Jing X, Mi HY, Turng LS. Comparison between PCL/hydroxyapatite (HA) and PCL/halloysite nanotube (HNT) composite scaffolds prepared by co-extrusion and gas foaming. Materials Science and Engineering: C. 2017; 72:53-61.

[9] Åkerlund E, Diez-escudero A, Grzeszczak A, Persson C. The effect of PCL addition on 3d-printable PLA/HA composite filaments for the treatment of bone defects. Polymers. 2022; 14(16):1-17.

[10] Kurniawan D, Nor FM, Lee HY, Lim JY. Elastic properties of polycaprolactone at small strains are significantly affected by strain rate and temperature. Proceedings of the Institution of Mechanical Engineers, Part H: Journal of Engineering in Medicine. 2011; 225(10):1015-20.

[11] Dwivedi R, Kumar S, Pandey R, Mahajan A, Nandana D, Katti DS, et al. Polycaprolactone as biomaterial for bone scaffolds: review of literature. Journal of Oral Biology and Craniofacial Research. 2020; 10(1):381-8.

[12] Gómez-lizárraga KK, Flores-morales C, Del prado-audelo ML, Álvarez-pérez MA, Piña-barba MC, Escobedo C. Polycaprolactone-and polycaprolactone/ceramic-based 3D-bioplotted porous scaffolds for bone regeneration: a comparative study. Materials Science and Engineering: C. 2017; 79:326-35.

[13] Mondal D, Griffith M, Venkatraman SS. Polycaprolactone-based biomaterials for tissue engineering and drug delivery: current scenario and challenges. International Journal of Polymeric Materials and Polymeric Biomaterials. 2016; 65(5):255-65.

[14] Wachirahuttapong S, Thongpin C, Sombatsompop N. Effect of PCL and compatibility contents on the morphology, crystallization and mechanical properties of PLA/PCL blends. Energy Procedia. 2016; 89:198-206.

[15] Kondiah PP, Rants'o TA, Mdanda S, Mohlomi LM, Choonara YE. A poly (caprolactone)-cellulose nanocomposite hydrogel for transdermal delivery of hydrocortisone in treating psoriasis vulgaris. Polymers. 2022; 14(13):1-23.
[16] Rahman MS, Hasan MS, Nitai AS, Nam S, Karmakar AK, Ahsan MS, et al. Recent developments of carboxymethyl cellulose. Polymers. 2021; 13(8):1-48.
[17] Zennifer A, Senthilvelan P, Sethuraman S, Sundaramurthi D. Key advances of carboxymethyl cellulose in tissue engineering & 3D bioprinting applications. Carbohydrate Polymers. 2021; 256:1-18.
[18] Gaihre B, Jayasuriya AC. Fabrication and characterization of carboxymethyl cellulose novel microparticles for bone tissue engineering. Materials Science and Engineering: C. 2016; 69:733-43.
[19] Qi P, Ohba S, Hara Y, Fuke M, Ogawa T, Ohta S, et al. Fabrication of calcium phosphate-loaded carboxymethyl cellulose non-woven sheets for bone regeneration. Carbohydrate Polymers. 2018; 189:322-30.
[20] Fan L, Peng M, Zhou X, Wu H, Hu J, Xie W, et al. Modification of carboxymethyl cellulose grafted with collagen peptide and its antioxidant activity. Carbohydrate Polymers. 2014; 112:32-8.
[21] Biswal DR, Singh RP. Characterisation of carboxymethyl cellulose and polyacrylamide graft copolymer. Carbohydrate Polymers. 2004; 57(4):379-87.
[22] Diaz-gomez L, Gonzalez-prada I, Millan R, Da SA, Bugallo-casal A, Campos F, et al. 3D printed carboxymethyl cellulose scaffolds for autologous growth factors delivery in wound healing. Carbohydrate Polymers. 2022; 278:1-12.
[23] Cheng J, Zhang LT. A general approach to derive stress and elasticity tensors for hyperelastic isotropic and anisotropic biomaterials. International Journal of Computational Methods. 2018; 15(4):1-40.
[24] Wiwatwongwana F, Chaijit S. Mechanical properties analysis of gelatin/carboxymethylcellulose scaffolds. International Journal of Materials, Mechanics and Manufacturing. 2019; 7(3):138-43.
[25] Holzapfel GA. Nonlinear solid mechanics: a continuum approach for engineering science. Meccanica. 2002; 37(4):489-90.
[26] Dong X, Duan Z. Comparative study on the sealing performance of packer rubber based on elastic and hyperelastic analyses using various constitutive models. Materials Research Express. 2022; 9(7):1-13.
[27] Anssari-benam A, Bucchi A, Saccomandi G. Modelling the inflation and elastic instabilities of rubber-like spherical and cylindrical shells using a new generalised neo-Hookean strain energy function. Journal of Elasticity. 2022; 151(1):15-45.
[28] Simon PFJ, Cuadrado SÓ, Marques EA, Sánchez LM, Da SLF. Mechanical characterisation and comparison of hyperelastic adhesives: modelling and experimental validation. Journal of Applied and Computational Mechanics. 2022; 8(1):359-69.
[29] Kar P, Myneni M, Tůma K, Rajagopal KR, Benjamin CC. Axial pulling of a neo-Hookean fiber embedded in a generalized neo-Hookean matrix. International Journal of Non-Linear Mechanics. 2022; 148:1-10.
[30] Chen Y, Guo W, Yang P, Zhao J, Guo Z, Dong L, et al. Constitutive modeling of neo-Hookean materials with spherical voids in finite deformation. Extreme Mechanics Letters. 2018; 24:47-57.
[31] Raheem HM, Al-mukhtar AM. Experimental and analytical study of the hyperelastic behavior of the hydrogel under unconfined compression. Procedia Structural Integrity. 2020; 25:3-7.
[32] Liu Y, Moran B. Effects of multiple families of nonlinear fibers on finite deformation near a crack tip in a neo-Hookean sheet. European Journal of Mechanics-A/Solids. 2021; 90:1-19.
[33] Plotnikov PI. Mathematical modeling of neo-Hookean material growth. Doklady Mathematics. 2021; 104(3):380-4. Pleiades Publishing.
[34] Zheng Y, Cai S. Analytical solutions of cavitation instability in a compressible hyperelastic solid. International Journal of Non-Linear Mechanics. 2020; 126(2020):1-6.
[35] Shao Z, Zhu M, Wang H, Li M. Effect of aging of foam rubber on properties and constitutive models. In journal of physics: conference series 2021 (pp. 1-5). IOP Publishing.
[36] https://www.nist.gov/system/files/documents/mml/bbd/biomaterials/Scaffold-Fabrication-Tutorial.pdf. Accessed 26 October 2020.
[37] Thadavirul N, Pavasant P, Supaphol P. Development of polycaprolactone porous scaffolds by combining solvent casting, particulate leaching, and polymer leaching techniques for bone tissue engineering. Journal of Biomedical Materials Research Part A. 2014; 102(10):3379-92.
[38] Phothiphatcha J, Puttapitukporn T. Determination of material parameters of PDMS material models by MATLAB. Engineering Journal. 2021; 25(4):11-28.
[39] Kim B, Lee SB, Lee J, Cho S, Park H, Yeom S, et al. A comparison among neo-Hookean model, mooney-rivlin model, and ogden model for chloroprene rubber. International Journal of Precision Engineering and Manufacturing. 2012; 13(5):759-64.
[40] Ogden RW. Large deformation isotropic elasticity–on the correlation of theory and experiment for incompressible rubberlike solids. Proceedings of the Royal Society of London. A. Mathematical and Physical Sciences. 1972; 326(1567):565-84.
[41] Berselli G, Vertechy R, Pellicciari M, Vassura G. Hyperelastic modeling of rubber-like photopolymers for additive manufacturing processes. Rapid Prototyping Technology-Principles and Functional Requirements, Hoque, M.(Ed.), IntechOpen Ltd., London. 2011:135-52.
[42] Łagan SD, Liber-kneć A. Experimental testing and constitutive modeling of the mechanical properties of the swine skin tissue. ACTA of Bioengineering and Biomechanics. 2017; 19(2):93-102.

[43] Wiwatwongwana F, Klunathon Y, Rangsri W, Promma N, Pattana S. Identification of shear modulus of gelatin blended with carboxymethylcellulose scaffolds using curve fitting method from compressive test. Journal of Materials Science Research. 2012; 1(4):106-13.
[44] Huang Y, Onyeri S, Siewe M, Moshfeghian A, Madihally SV. In vitro characterization of chitosan–gelatin scaffolds for tissue engineering. Biomaterials. 2005; 26(36):7616-27.
[45] Lien SM, Ko LY, Huang TJ. Effect of crosslinking temperature on compression strength of gelatin scaffold for articular cartilage tissue engineering. Materials Science and Engineering: C. 2010; 30(4):631-5.
[46] Harley BA, Leung JH, Silva EC, Gibson LJ. Mechanical characterization of collagen–glycosaminoglycan scaffolds. ACTA Biomaterialia. 2007; 3(4):463-74.

Noppadol Sriputtha was born on December 26, 1971 in Khonkaen Province, Thailand. About his education, he is an Engineering Ph.D. candidate in Advanced Manufacturing Technology at Pathumwan Institute of Technology in Bangkok, Thailand. He graduated with a Master of Industrial Engineering in May 2010 from Chulalongkorn University, Bangkok, Thailand, a Master of Engineering in Industrial Management Engineering in October 2003 from King Mongkut's Institute of Technology North Bangkok, Bangkok, Thailand, and a Bachelor of Production Technology in March 2000 King Mongkut's Institute of Technology North Bangkok, Bangkok, Thailand. He has teaching experience as a lecturer in Department of Robotics and Lean Automation Engineering and Department of Production Engineering, Faculty of Engineering, Thai-Nichi Institute of Technology, from September 2012 to present. He also has more than 25 years of hands-on experience in the manufacturing industry.
Email: idol7877@gmail.com

Fasai Wiwatwongwana was born on November 5, 1982 in Chiang Mai Province, Thailand. About her education, she graduated Ph.D. of Mechanical Engineering in December 2012 from Chiang Mai University, Chiang Mai, Thailand, Master of Chemical Engineering in April 2007 from Chulalongkorn University, Bangkok, Thailand and Bachelor of Engineering, Chemical Engineering in April 2004 from Thammasat University, Bangkok, Thailand. She has teaching experiences as a lecturer at Department of Advanced Manufacturing Technology and Department of Manufacturing Engineering, Faculty of Engineering, Pathumwan Institute of Technology from June 2014 to present, Department of Mechanical Engineering, Faculty of Engineering, Rajamangala University of Technology Lanna Chiang Mai from June 2013 to May 2014 and Biomedical Engineering Program (International Program), Graduate School, Chiang Mai University from June 2009 to May 2013. She also has experience as a researcher at the Biomedical Engineering Center, Chiang Mai University from March 2008 to May 2013 and the Center for Agricultural Biotechnology, Faculty of Agriculture, Chiang Mai University from July 2007 to February 2008.
Email: fasaiw227@gmail.com

Nattawit Promma was born on July 15, 1977 in Chiang Mai Province, Thailand. About his education, he received his Bachelor degree of Mechanical Engineering in May 1999 and Master of Energy Engineering in October 2001 from Chiang Mai University, Chiang Mai, Thailand. After graduation, he was employed under the position of engineer by Fujikura Thailand Co., Ltd. for 4 months. He served in the position of lecturer at the Department of Mechanical Engineering, Faculty of Engineering, Chiang Mai University in 2002. His phone number is +66-5394-4145 ext. 936 and mobile number is +66-81-536-4244. In 2009, he graduated Ph.D. of Mechanical Engineering in April 2009 from Blaise Pascal University - Clermont Ferrand II, France. He is an assistant professor in Mechanical Engineering at Department of Mechanical Engineering, Faculty of Engineering, Chiang Mai University at present.
Email: nano_504@hotmail.com

Appendix I

S. No.	Abbreviation	Description
1	3D	Three-Dimensional
2	CMC	Carboxymethylcellulose
3	DI	Deionized
4	ECM	Extracellular Matrix
5	FEA	Finite Element Analysis
6	FEM	Finite Element Model
7	HNBR	Hydrogenated Nitrile Butadiene Rubber
8	Mm	Millimeter
9	MPa	Mega Pascal
10	Mw	Molecular Weight
11	NaCl	Sodium Chloride
12	PCL	Polycaprolactone
13	PLLA	Poly-l-Lactic Acid
14	PLGA	Polylactic Glycolic Acid
15	RSS	Residual Sum of Squares
16	SD	Standard Deviation
17	TE	Tissue Engineering
18	TFE	Trifluoroethanol
19	UTM	Universal Testing Machine